Shot-by-shot imaging of Hong–Ou–Mandel interference with an intensified sCMOS camera

Michał Jachura and Radosław Chrapkiewicz*

Faculty of Physics, University of Warsaw, Pasteura 5, 02-093 Warsaw, Poland *Corresponding author: radekch@fuw.edu.pl

Received January 26, 2015; revised March 2, 2015; accepted March 3, 2015; posted March 5, 2015 (Doc. ID 232669); published March 30, 2015

We report the first observation of Hong–Ou–Mandel (HOM) interference of highly indistinguishable photon pairs with spatial resolution. Direct imaging of two-photon coalescence with an intensified sCMOS camera system clearly reveals spatially separated photons appearing pairwise within one of the two modes. With the use of the camera system, we quantified the number of pairs and recovered the full HOM dip yielding 96.3% interference visibility, as well as counted the number of coalesced pairs. We retrieved the spatial modes of both interfering photons by performing a proof-of-principle demonstration of a new, low-noise, high-resolution coincidence imaging scheme. © 2015 Optical Society of America

OCIS codes: (030.5260) Photon counting; (040.1490) Cameras; (270.5570) Quantum detectors; (270.0270) Quantum optics.

http://dx.doi.org/10.1364/OL.40.001540

Recent advances in single-photon-sensitive cameras such as electron multiplying and intensified charged coupled devices (EMCCD and ICCD) have substantially stimulated the exploration of optical phenomena at the lowintensity levels [1]. In particular, camera systems were successfully applied in quantum optics for the observation of the entanglement between the position and the momentum known as Einstein-Podolsky-Rosen correlations [2,3] or between optical angular momentum modes [4] as well as for investigation of the spatial correlations in spontaneous parametric down-conversion (SPDC) [5–7]. They have also been used to demonstrate a variety of intriguing quantum-enhanced techniques including ghost imaging [8], quantum imaging of object with undetected photons [9], and sub-shot noise imaging [10]. Nevertheless, a vast majority of the aforementioned experiments still typically operate in the regime of several to hundreds of photons per camera frame. Experiments with truly single pairs of photons have been virtually out of the grasp of the cameras due to their slow frame rate and high noise, therefore the pioneer works dating back to more than a decade ago [6,11] have not lived to see their direct followers, and the methods for realizing spatially resolved coincidence measurements were based on scanning single-pixel detectors [12] or detector arrays reaching a dozen of pixels [13].

In this Letter, we extend the possible applications of the camera systems to the observation of single pairs of photons by the successful recording of two-photon Hong-Ou-Mandel (HOM) interference [14]. This prominent quantum optical effect has been studied so far only using area-integrating detectors [15]. Utilizing a novel intensified sCMOS camera system, sketched in Fig. 1(a), we are able to image effectively, shot-by-shot, the photon coalescence effect with high-spatial resolution. We also quantify the number of two-photon events using natural photon-number-resolving capability of our system and demonstrate full recovery of HOM dip yielding the visibility in perfect agreement with an independent measurement performed by the standard avalanche photodiodes (APDs) coincidence setup. High visibility of the obtained HOM dip confirms both the excellent signal-to-noise ratio of our detection system and the indistinguishability of interfering photons spatial modes that have been additionally retrieved in the extended coincidence imaging scheme.

We observe the photons on the single-photon-sensitive intensified sCMOS camera system assembled from commercially available components, the scheme of which is shown in Fig. 1(a). The photons illuminate directly the image intensifier (Hamamatsu V7090D) of a quantum efficiency of 23%. Inside the intensifier, each photon that induces a photoelectron emission produces a macroscopic charge avalanche resulting in a bright flash at the output phosphor screen that is imaged with a high numerical aperture relay lens on the fast, low-noise sCMOS sensor (Andor Zyla). The flashes detected at the sCMOS as 25-pixel Gaussian spots can be easily discriminated from the low-noise background. Remarkably, in our setup, the number of thermally induced events was negligible, and thus virtually all of the registered events could be associated with incoming photons. Their central positions x_i , y_i are retrieved from each captured frame with a subpixel resolution, as sketched in Fig. 1(b), by a real-time software algorithm designed in our group [16]. In the experiment, we restrain the data flow by preselecting the two-photon detection events, although it can be readily extended to the multi-photon imaging regime, as exemplified in [16].

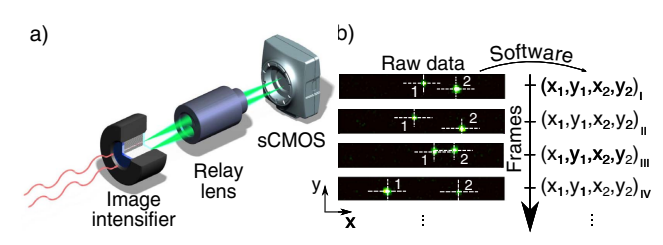


Fig. 1. (a) Scheme of the intensified sCMOS camera detection system. (b) Single-photon detection seen as bright phosphore flashes are localized with a subpixel resolution using the real-time processing software algorithm. We preselect events where at least two photons are detected.

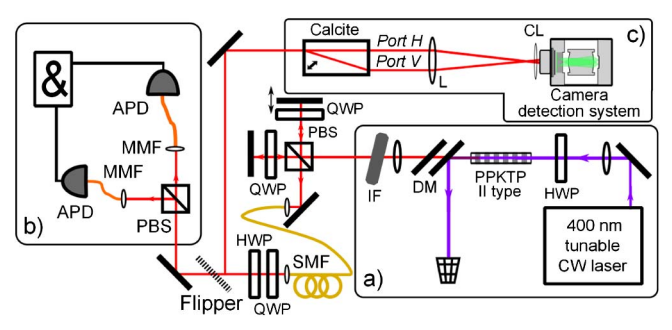


Fig. 2. Experimental setup for generation and spatially resolved detection of highly indistinguishable photon pairs. (a) Photon pair source based on SPDC in type-II PPKTP crystal, followed by the optical delay line. (b) Standard avalanche photodiodes coincidence setup. (c) Calcite beam displacer imaged onto the front surface of the camera detection system described in Fig. 1(a). HWP, QWP—half- and quarter-wave plates, PBS—polarizing beam splitter, MMF—multimode fiber, DM—dichroic mirrors. See text for further details.

The majority of detected two-photon events originate from single photon pairs; however, they cannot be distinguished from those generated by two photons from two independent pairs. The latter, accidental coincidences decrease the registered visibility of two-photon interference and thus have to be suppressed. Since their number scales quadratically with the gating time, we could trade off their contribution with pair detection probability that scales up linearly. We empirically found the suitable gating time of 40 ns, which, as we show further, satisfies the aforementioned conditions. The gating pulses were provided externally by the digital pulse generator (Stanford DG-645).

In our experimental setup depicted in Fig. 2, we utilize the source of photon pairs based on the type-II SPDC process realized in a 5-mm-long periodically poled KTP (PPKTP) crystal that is pumped by 8 mW of 400-nm continuous wave diode laser, as presented in Fig. 2(a). To ensure high visibility of the two-photon interference, we erase any residual distinguishability of photons inside each pair with respect to the spectral, temporal, and spatial degree of freedom, which is consecutively realized by a narrowband 3-nm FWHM interference filter (IF), an optical delay line, and a single-mode fiber (SMF). The photons are either directed to the standard APD coincidence setup, shown in Fig. 1(b), or separated by means of the 30-mm-long calcite beam displacer whose rear surface is imaged onto the camera detector as seen in Fig. 1(c). Using the APD configuration, we detect approximately 11,000 pairs/s, which results in a coincidence to single counts ratio of 15%. The SMF followed by the calcite crystal defines two orthogonally polarized Gaussian-like modes separated by 3.2 mm.

The positions of photons at the calcite surface are mapped onto the $6.5 \ \mu m \times 6.5 \ \mu m$ pixel size sCMOS sensor with a magnification of M=1.1 in horizontal direction. We placed a cylindrical lens (CL) f=30 mm in front of the detector to reduce the vertical size of the image, thus significantly decreasing the frame readout time. We collect the data from a $700 \ px \times 22 \ px$ stripe with a frame rate of 7 kHz using approximately $9 \times 10^4 \ microchannels$ of the image intensifier, each acting as a binary

single-photon detector. During the experiment, we noticed that the photoelectron multiplication can trigger another avalanche in the neighboring channel, hence we had to reject the events where the distance between photons including both directions were smaller than twelve pixels of sCMOS detectors.

In the experiment, we set the polarization angle of orthogonally polarized photon pair to 45° with respect to the basis defined by the calcite beam displacer, which then acts effectively as a balanced beam-splitter. Ideally, it leads to the perfect HOM interference where outgoing photons coalesce upon leaving the displacer together in one of the two available output modes [14]. This effect has usually been observed indirectly on area-integrating detectors as a decrease in the number of coincidence events between the two different output ports [17].

Here, thanks to the high resolution of our detection system, we are able to spatially resolve two coalesced photons within the transversal mode they occupy. It has been presented in the recorded movie, which is included in Media 1, and in Fig. 3 we present its exemplary frames. At first in Fig. 3(a), we present the situation where photons are temporarily distinguishable, and they appear in output modes H and V in each possible configuration. In Fig. 3(b), we set the delay line so as to remove temporal distinguishability, and the HOM interference occurs. In all but one of the presented frames, the photons were detected in the same output port exhibiting excellent two-photon coalescence, and we clearly see that photon pairs randomly appear in separated positions within the mode

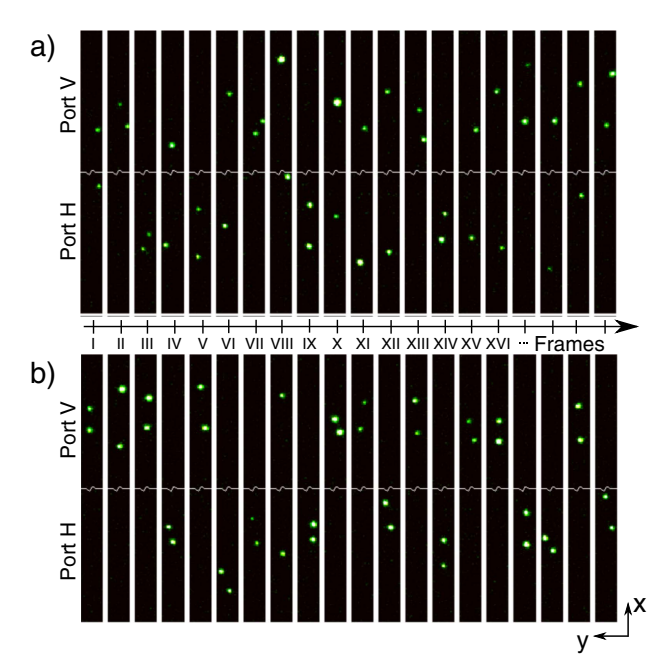


Fig. 3. The 20 frames excerpts from the movie presenting the image of the rear surface of the calcite beam displacer. For a better visualization, we display only the area corresponding to the area of output modes H and V. (a) Distinguishable photons do not interfere and exit output ports in each configuration: HH, VV, and HV. (b) Hong–Ou–Mandel interference of indistinguishable photons clearly manifests itself as nearly perfect two-photon coalescence visible as grouping of photons in pairs in HH or VV configurations in all but one of the presented frames (Media 1).

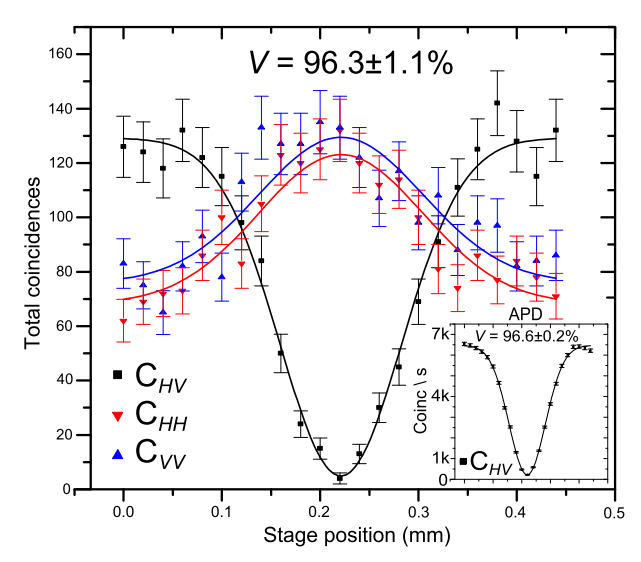


Fig. 4. Recovery of the HOM-dip from the coincidences between ports $C_{\rm HV}$ measured by means of a camera system along with photon pairs detected at single output ports $C_{\rm HH}$, $C_{\rm VV}$. Inset: the analogous result $C_{\rm HV}$ obtained using the avalanche photo diodes setup.

area. Even in such a small excerpt presented in Fig. 3(b), we observe that the number of coincidence is uniformly distributed between two regions, which also agrees with theoretical predictions.

We perform a final verification of the visibility of recorded two-photon interference by a full recovery of the HOM dip. Remarkably for such a measurement, we can also employ our detection system and exploit its photon-number-resolving capability to directly count the photon pairs at each output port of the calcite beam displacer. We measure the total number of two-photon events inside either of the two output ports C_{VV} , C_{HH} along with registering a single photon in each region $C_{\rm HV}$, with respect to the delay line position, as shown in Fig. 4. For each delay line position, we collected 5×10^6 frames. We achieved a visibility of HOM interference as high as $96.3 \pm 1.1\%$, which is comparable to the state of the art for the sources based on the bulk PPKTP crystals [18]. The results are in excellent agreement with the independent measurement performed using a standard APDs setup, see Fig. 4 (inset), which yielded $96.6 \pm$ 0.2%. Furthermore, the photon coalescence effect can be clearly recognized from the number of $C_{\rm HH}$, $C_{\rm VV}$ events with respect to the delay line shift. The total number of counts reflects the theory, which predicts $C_{\rm HH} =$ $C_{\text{VV}} = \frac{1}{2}C_{\text{HV}}$ for distinguishable photons (outside the dip) and $C_{\rm HV} = 0$, $C_{\rm HH} = C_{\rm VV}$ for perfectly indistinguishable photons (inside the dip) [15]. Differences between $C_{\rm HH}$ and C_{VV} can be explained by unequal transmission through the uncoated calcite crystal. The explicit measurement of the photon coalescence, i.e., C_{VV} , C_{HH} , has been performed so far using ultra-low-temperature transition-edge superconducting detectors [15].

Utilizing the coordinates of detected photons positions, we can retrieve the spatial modes they occupy, which additionally verifies their indistinguishability, indispensable for high-visibility HOM interference measured on a large-area sensor. The problem of measuring a single photon transversal mode reoccurs in numerous experiments, and it is commonly tackled with the coincidence imaging schemes where raw ICCD images, conditioned on a heralding photon detected by a bucket detector, are simply averaged out [4] or alternatively approached with knife-edge methods [19]. Here we propose and demonstrate the extended single-device scheme that avoids cumbersome optical delay lines [20] and keeps hitherto unaccessible spatial information about heralding photon.

In particular, we measure two spatial modes of orthogonally polarized photons by adjusting their polarizations to the calcite beam displacer basis. For this setting, the detection of photon in port H heralds the photon in port V and vice versa, as seen in Fig. 5(a), thus each of detected photons can be associated with one of the spatial modes it occupies. We take into account the coordinates of their central positions, shown in Fig. 5(b), ascribing equal weight to each of the registered detection events. The two-dimensional histogram of positions of the 5100 detected pairs of photons, presented in Fig. 5(c), clearly reveals the structure of the modes. Remarkably, the resolution of the image is well below the image intensifier flash size, and the shot noise of the number of counts at each histogram bin mitigates the thermal noise of the raw image intensifier response present in a traditional coincidence imaging scheme. Although for the proof-of-principle purposes we stick to the simple Gaussian-like modes, the presented scheme can be readily applied to more complex spatial modes, including the frequently used OAM basis [4].

In conclusion, we presented a spatially resolved observation of the HOM interference complemented by the full recovery of HOM dip along with the direct observation of photon pairs at a single output port. All results were obtained with application of intensified sCMOS camera system to the detection of light at the truly single-photon level. High visibility of the measured two-photon interference is the evidence for a high signal-to-noise ratio of our system, which is indispensable for the majority of quantum imaging applications. We also proposed an extended version of a coincidence imaging schemes based on spatially resolved detection of two mutually heralding

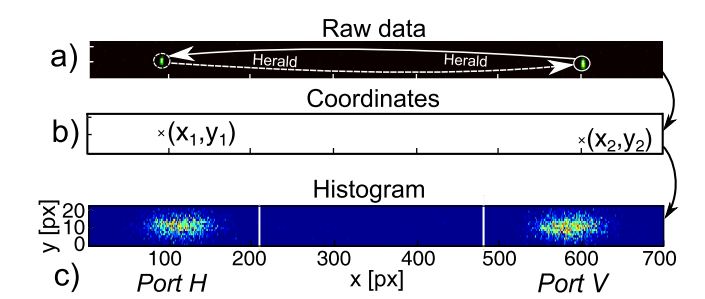


Fig. 5. Proof-of-principle demonstration of the coincidence imaging of single-photon modes without bucket detectors, where both photons from each detected pair, initially orthogonally polarized and displaced into two independent modes, herald each other (a). Their positions are converted in real time into plain coordinate data (b) which are then accumulated into a histogram of approximately 5000 coincidence events revealing spatial mode structure of detected photons (c).

photons and performed its proof-of-principle demonstration for retrieving the spatial modes of both interfering photons.

We believe that our work and presented concepts are valuable steps toward the exploration of spatial correlation exhibited by non-classical light generated in photonic [3] and atomic systems [21], building quantumenhanced super-resolution imaging systems [13], development of optical nanoscopy [1], as well as easier characterization of the single-photon spatial-mode structure [19]. We anticipate that intensified cameras, besides the cryogenic nanowires [22], are among the most promising technologies for high spatial resolution detection of single- and multi-photon events due to their low noise, high filling factor, and short gating time. Further technical progress involving the time-stamp functionality [23], increase in quantum efficiency, and direct electronic readout of the charge from the microchannel plate would make this technique even more powerful.

We acknowledge the support and discussions with K. Banaszek, J. Iwaszkiewicz, M. Karpiński, M. Niemiec, and W. Wasilewski. This project was financed by the National Science Centre projects no. DEC-2013/09/N/ST2/02229 and DEC-2011/03/D/ST2/01941.

References

- 1. V. Krishnaswami, C. J. Van Noorden, E. M. M. Mander, and R. A. Hoebe, Opt. Nanosc. 3, 1 (2014).
- M. P. Edgar, D. S. Tasca, F. Izdebski, R. E. Warburton, J. Leach, M. Agnew, G. S. Buller, R. W. Boyd, and M. J. Padgett, Nat. Commun. 3, 984 (2012).
- P.-A. Moreau, F. Devaux, and E. Lantz, Phys. Rev. A 113, 160401 (2014).
- R. Fickler, M. Krenn, R. Lapkiewicz, S. Ramelow, and A. Zeilinger, Sci. Rep. 3, 1914 (2013).
- B. Jost, A. Sergienko, A. Abouraddy, B. Saleh, and M. Teich, Opt. Express 3, 81 (1998).

- S. S. R. Oemrawsingh, W. J. van Drunen, E. R. Eliel, and J. P. Woerdman, J. Opt. Soc. Am. B 19, 2391 (2002).
- R. Machulka, O. Haderka, J. Peřina, M. Lamperti, A. Allevi, and M. Bondani, Opt. Express 22, 13374 (2014).
- A. Gatti, E. Brambilla, and L. Lugiato, Prog. Opt. 51, 251 (2008).
- 9. G. B. Lemos, V. Borish, G. D. Cole, S. Ramelow, R. Lapkiewicz, and A. Zeilinger, Nature **512**, 409 (2014).
- G. Brida, M. Genovese, and I. R. Berchera, Nat. Photonics 4, 227 (2010).
- A. F. Abouraddy, M. B. Nasr, B. E. A. Saleh, A. V. Sergienko, and M. C. Teich, Phys. Rev. A 63, 63803 (2001).
- H. Shin, K. W. C. Chan, H. J. Chang, and R. W. Boyd, Phys. Rev. A 107, 083603 (2011).
- L. A. Rozema, J. D. Bateman, D. H. Mahler, R. Okamoto, A. Feizpour, A. Hayat, and A. M. Steinberg, Phys. Rev. A 112, 223602 (2014).
- C. K. Hong, Z. Y. Ou, and L. Mandel, Phys. Rev. A 59, 2004 (1987).
- G. Di Giuseppe, M. Atatüre, M. Shaw, A. Sergienko, B. Saleh, M. Teich, A. Miller, S. Nam, and J. Martinis, Phys. Rev. A 68, 063817 (2003).
- R. Chrapkiewicz, W. Wasilewski, and K. Banaszek, Opt. Lett. 39, 5090 (2014).
- M. Jachura, C. Radzewicz, M. Karpiński, and K. Banaszek, Opt. Express 22, 8624 (2014).
- C. Kuklewicz, M. Fiorentino, G. Messin, F. Wong, and J. Shapiro, Phys. Rev. A 69, 013807 (2004).
- M. Karpiński, C. Radzewicz, and K. Banaszek, Opt. Lett. 37, 878 (2012).
- P. A. Morris, R. S. Aspden, J. E. C. Bell, R. W. Boyd, and M. J. Padgett, Nat. Commun. 6, 5913 (2015).
- M. Dąbrowski, R. Chrapkiewicz, and W. Wasilewski, Opt. Express 22, 26076 (2014).
- E. A. Dauler, M. E. Grein, A. J. Kerman, F. Marsili, S. Miki,
 S. W. Nam, M. D. Shaw, H. Terai, V. B. Verma, and T. Yamashita, Opt. Eng. 53, 081907 (2014).
- 23. J. J. John, M. Brouard, A. Clark, J. Crooks, E. Halford, L. Hill, J. W. L. Lee, A. Nomerotski, R. Pisarczyk, I. Sedgwick, C. S. Slater, R. Turchetta, C. Vallance, E. Wilman, B. Winter, and W. H. Yuen, J. Instrum. 7, C08001 (2012).